JOURNAL OF QUATERNARY SCIENCE (2024) 1–11 ISSN 0267-8179. DOI: 10.1002/jqs.3590

JQS Journal of Quaternary Science QRA Quaternary Research Association

Vertical acoustic blanking in seismic data from the German North Sea: a spotlight to shallow gas-bearing incised channels

NIKLAS AHLRICHS,[1]* AXEL EHRHARDT,[1] MICHAEL SCHNABEL[1] and CHRISTIAN BERNDT[2]
[1]Federal Institute for Geosciences and Natural Resources (BGR), Hannover, Germany
[2]Geomar Helmholtz-Zentrum für Ozeanforschung Kiel, 24148 Kiel, Germany

Received 24 August 2023; Revised 28 November 2023; Accepted 7 December 2023

ABSTRACT: Seismic data from the North Sea commonly show vertical acoustic blanking (VAB) often interpreted as fluid conduits with implications for Quaternary development. The robustness of this interpretation has long been controversial as the infill of tunnel valleys can also cause vertical blanking. Using 2D and 3D seismic data and sediment echosounder data from the German North Sea, we investigate VAB to determine a geological or imaging origin of these anomalies. We detected multiple VAB occurrences throughout the North Sea. 3D data from the Ducks Beak ('Entenschnabel') reveal a correlation of VAB with bright spots in incised channels directly below the seafloor. Large source–receiver distances allow imaging the subsurface below the channel without signal penetrating through it (undershooting). This method removes the blanking. Energy absorption by shallow biogenic gas trapped within the channels explains the observed VAB. Hence, the blanking represents an imaging artifact, highlighting the need for careful seismic processing with sufficient offset before interpreting such anomalies as fluid pathways. The channels belong to a postglacial channel system related to the now submerged lowlands of Doggerland. This work demonstrates the usability of mapping VAB to detect shallow features for paleo-landscape reconstruction and identification of shallow gas for hazard assessments, for example.

KEYWORDS: North Sea; postglacial fluvial channels; Quaternary; seismic imaging artifacts; shallow gas

Introduction

The interpretation of reflection seismic data plays a vital role in identifying subsurface structures. One crucial aspect in this regard is linking observable features in seismic images to their corresponding geology. In addition to travel time and the characteristics of reflections, irregularities in the seismic image are key elements for identifying seismic expressions of geological structures such as faults and fluid migration pathways. The latter can be identified using local discontinuities in the reflection pattern, amplitude anomalies and phase reversals. The identification of such features is of great importance in various fields, including exploration for subsurface CO_2 or hydrogen storage as well as hydrocarbon exploration. Within this context, areas with a vertically disrupted, chaotic reflection pattern and attenuated amplitude are often interpreted as indicative of a fluid conduit such as gas chimneys. In the North Sea, this is often observed at faults related to salt structures (Schroot and Schüttenhelm, 2003; Müller et al., 2018; Callow et al., 2021) or related to fluid ascent from the deeper subsurface (Karstens and Berndt, 2015; Böttner et al., 2019). However, shallow structures such as tunnel valleys or fluvial channels, potentially with a gas-charged sedimentary infill, may have similar effects on the seismic record resulting in masking of the underlying true geological structures (Judd and Hovland, 1992; Armstrong et al., 2001; Schroot and Schüttenhelm, 2003; Kristensen et al., 2012; Karstens and Berndt, 2015; Callow et al., 2021; de Bruin et al., 2022).

One commonly observed anomaly in North Sea seismic data is the occurrence of patches of vertical acoustic blanking (VAB) beneath surficial bright spots (Figure 1). In these cases, the seismic signal is strongly attenuated, reflections are discontinuous and no clear image of the subsurface can be obtained (Judd and Hovland, 1992). Such locally confined acoustic blanking or the presence of chaotic reflections described as acoustic turbidity is a known phenomenon in hydroacoustic and seismic data, for examplein the Black Sea, Baltic Sea or modern rivers, and is attributed to shallow gas-charged sediment (Okyar and Ediger, 1999; Garcia-Gil et al., 2002; Mathys et al., 2005; Laier and Jensen, 2007; Tóth et al., 2014). In the German North Sea, investigations of shallow gas as a potential energy resource detected multiple acoustic anomalies (Trampe et al., 2014), but the exact origin and differentiation between shallow anomalies and fluid conduits in the North Sea is not well understood. This study aims to determine whether these VAB features can be related to fluid conduits coming from the deeper subsurface, and thus if these features represent the seismic expression of genuine geological structures or if the blanking is merely a seismic artifact masking underlying signal.

By systematically analyzing and mapping VAB anomalies across the German North Sea sector, using both industry and academic 2D and 3D seismic data acquired over the past decades, this study seeks to shed light on the nature of these anomalies. The investigation is complemented by recently acquired high-resolution 3D seismic data, allowing for a detailed examination of the shallow subsurface immediately below the seafloor, in combination with sediment echosounder data. The findings of this study will contribute to a better understanding of acoustic blanking in seismic data, helping to

*Correspondence: Niklas Ahlrichs, as above.
Email: niklas.ahlrichs@bgr.de

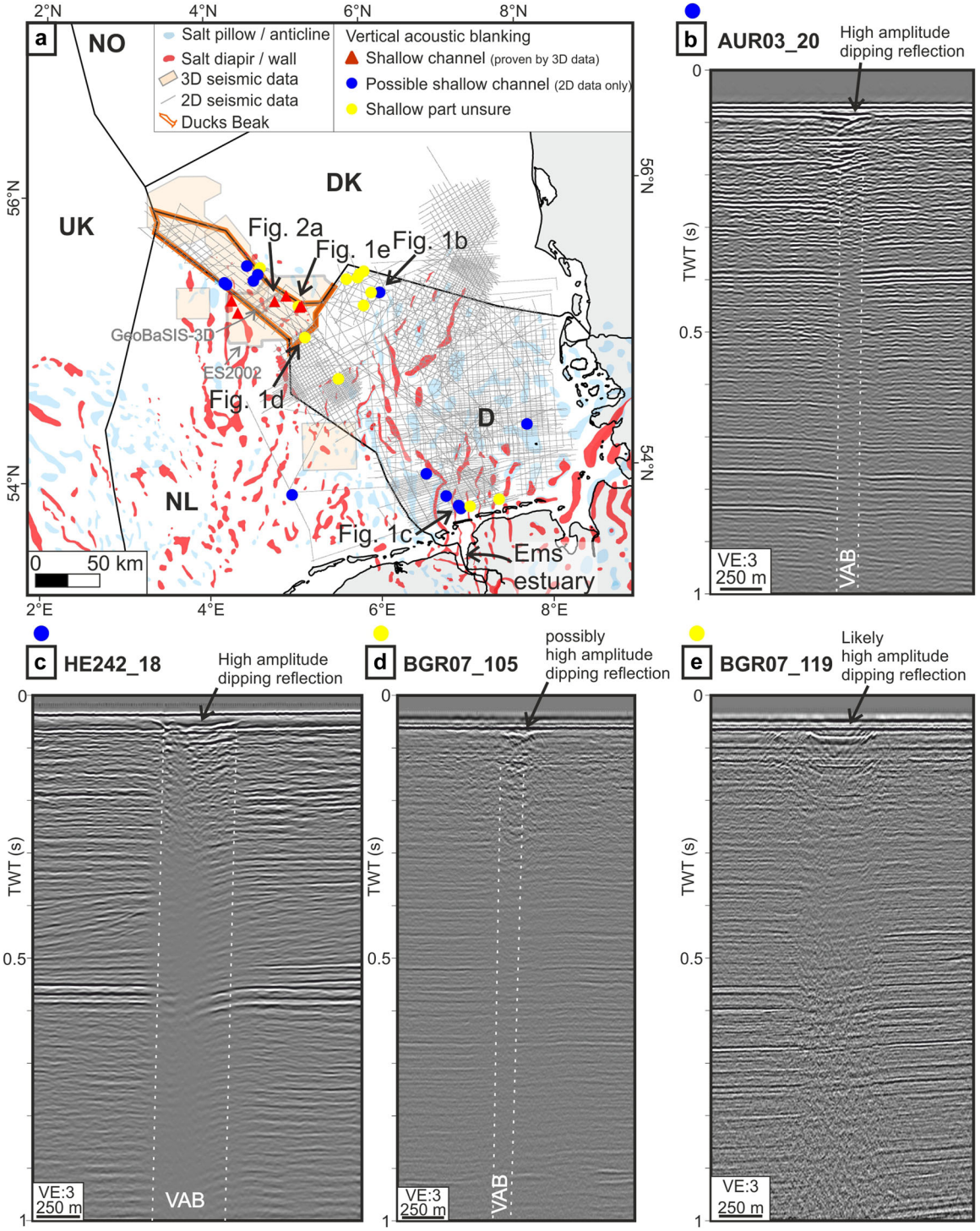

Figure 1. Vertical acoustic blanking across the German North Sea. (a) Map showing seismic database and identified VAB occurrences observed in industry and academic 2D and 3D seismic data. Color-coded circles mark locations of VAB. Classification based on their relationship with shallow channels. Important 3D seismic surveys GeoBaSIS-3D and ES2002 are labeled in grey (see 'Materials and methods' for further details. (b–e) Four representative examples of VAB visible in 2D seismic data. Images of all further identified VAB occurrences are included in Supporting Information S2 of this article. [Color figure can be viewed at wileyonlinelibrary.com]

avoid misinterpretation of such features as gas chimneys. This improved understanding will benefit investigations related to fluid migration, particularly in the context of carbon capture and storage (CCS) or other applications involving underground utilization.

Geological setting

The study area comprises the German North Sea sector and neighboring areas (Figure 1). The geological evolution of the German North Sea sector has been shaped by continental rifting, tectonic inversion and salt tectonics since Mesozoic times (Ziegler, 1990; Pharaoh et al., 2010; Warsitzka et al., 2019). As part of the Southern Permian Basin, the German North Sea sector was covered by the Zechstein Sea in late Permian times leading to the deposition of a thick evaporate succession (Tucker, 1991; Peryt et al., 2010). Subsequently, Triassic and Jurassic rifting caused intensive subsidence and structural differentiation (Ziegler, 1990; Underhill and Partington, 1993; Bachmann et al., 2010). The following post-rift phase is characterized by thermal subsidence in the Cretaceous and

Cenozoic. During this time, a thermal sag-basin was formed with thick deposition of sediments from the surrounding landmasses. Throughout the Cretaceous and Cenozoic, deposition was periodically interrupted by basin inversion causing uplift, erosion and fault reactivation (Ziegler, 1990; Vejbaek and Andersen, 2002; de Jager, 2003; Kley and Voigt, 2008; Pharaoh et al., 2010; Ahlrichs et al., 2021). During the Miocene, the southern North Sea became a significant depocenter with a westward prograding depositional system known as the Eridanos delta. Sediment supply to this area was delivered primarily by the Baltic River System (Cameron et al., 1993; Overeem et al., 2001; Thöle et al., 2014).

Since Mid-Pleistocene times, the North Sea sector has experienced three major glaciations (Elsterian, Saalian and Weichselian) during which large ice sheets covered much of the area. Only during the Last Glacial Maximum, in the Weichselian glaciation, did a significant portion of the southern North Sea remain ice-free. Glacial erosion during the cyclical ice advance and retreat alongside drainage of meltwater incised multiple tunnel valleys into the North Sea subsurface, which were filled with mostly tills, sand and clay (Ehlers, 1990; Huuse and Lykke-Andersen, 2000; Lutz et al., 2009; Hughes et al., 2016). Thereby, tunnel valley geometry and infill may be the result of a single or multiple ice advances and corresponding episodes of erosion and deposition (Piotrowski, 1994; Breuer et al., 2023). In the late Weichselian and early Holocene, a landmass called Doggerland emerged between Britain and the European mainland due to the falling sea-level. Doggerland, which was exposed between ~16 000 and 8000 years ago, featured a periglacial to fluvial environment comprising a riverine grassland landscape with lakes and wetlands, providing habitat for Mesolithic hunter-gatherer communities (Gaffney et al., 2009). Incised-fluvial channels are present across the entire North Sea and interpreted as the Doggerland drainage system draining into the Elbe Paleovalley (Gaffney et al., 2009; van Heteren et al., 2014; Hepp et al., 2017; Prins and Andresen, 2019). Subsequently, the Holocene transgression caused the area to be reflooded, leading to the formation of the modern seabed (Behre, 2007). The present-day sediments in the North Sea predominantly consist of shallow-marine, mostly mobile, sands (Zeiler et al., 2008).

Materials and methods

The multichannel reflection seismic data utilized in this study were acquired through a series of surveys conducted over the past few decades, encompassing both academic and industry efforts. The comprehensive database comprises 35 150 km of 2D data and 10 000 km^2 of 3D data, with the latter primarily covering the Ducks Beak area (Figure 1). Supporting Information S1 provides a summary of the varying acquisition parameters employed. The surveys were conducted between 1974 and 2020 and have variable data quality due to different acquisition setups, processing and technical improvements over time.

In 2021, the Federal Institute for Geoscience and Natural Resources (BGR), in collaboration with partner institutions, conducted a 94-km^2 3D seismic survey within the Ducks Beak in the framework of the GeoBaSIS-3D project. For this newly acquired dataset, an optimized acquisition setup was used yielding a broad signal spectrum and small initial offsets (Ehrhardt et al., 2021). These factors facilitated continuous and high-resolution imaging from the seafloor down to deeper buried Triassic and Zechstein deposits. Two streamer cables with an active length of 1050 m each recorded the signal from two GI Guns fired in flip-flop mode. The sampling rate was set to 1 ms, and the signal has a broadband spectrum with a dominant frequency bandwidth of 70–150 Hz. Seismic processing steps encompassed SRME multiple attenuation, frequency filtering, amplitude recovery, noise reduction, velocity analysis and prestack time migration.

The available 3D seismic data are used to investigate and map shallow incised channels directly below the seafloor. Thereby, the channels are represented by meandering trajectories with distinctive amplitude differences to neighboring areas (Figure 2).

Additionally, sediment echosounder data collected during the GeoBasSIS-3D cruise provided valuable insights into the uppermost sedimentary layers, reaching depths of ~40 m. The Atlas PARASOUND system DS P70 was used to record the data, utilizing primary frequencies of 18 and 22 kHz. Due to the lack of shallow sediment cores, stratigraphic interpretation of the sediment echsounder data is based on the characteristic reflection patterns and compared to published nearby sections and sediment cores (Hepp et al., 2017; Coughlan et al., 2018).

To identify VAB occurrences, all available seismic profiles were analyzed. Here, VAB refers to locally constrained patches of strongly attenuated amplitude and discontinuous reflections. The observed localities were mapped and classified based on their characteristics and correlation with shallow channel structures as well as the data quality imaging the anomalies. The introduced categorization includes: (i) VAB occurrences that correlate with a shallow channel structure confirmed by 3D data; (ii) VAB occurrences that correlate with a possible shallow channel, albeit solely imaged by 2D data; and (iii) situations where the shallow section above the VAB exhibits poor imaging hampering the correlation to potential shallow structures (Figure 1).

Results

VAB distribution and appearance

The comprehensive database utilized in this study revealed 30 occurrences of VAB distributed across the North Sea (Figure 1). The observed VAB patches exhibit varying widths ranging from 100 to 800 m and predominantly affect the seismic record from directly below the seafloor to 1–2 s two-way travel time (TWT) (Figure 1, all other identified occurrences are provided in Supporting Information S2). In cases where the shallow subsurface is well resolved, these patches often correlate with valley-like structures characterized by slightly dipping high-amplitude reflections (Figure 1b, c). However, in certain instances, the uppermost part of the seismic image is poorly resolved hampering a clear correlation to any shallow feature because of large near-channel distances and corresponding stretch mutes in the shallow water depth setting of the North Sea (Figure 1d). In principle, the VAB patches cluster within two regions: the first is located in the southwestern part of the German North Sea sector, in the northern prolongation of the Ems estuary, while the second is situated in the southeastern part of the Ducks Beak and northern German North Sea close to the Danish maritime border (Figure 1).

ILINE 409 from the GeoBaSIS-3D dataset shows a prominent, roughly 500-m-wide patch of VAB, which correlates with a well-resolved high-amplitude and NE-dipping reflection directly below the seafloor (Figure 2a). Notably, this high-amplitude reflection is located within a wider and deeper incising tunnel valley (highlighted by the yellow dotted line in Figure 2a). Further analysis using a time slice at 98 ms TWT reveals a clear correlation between the identified VAB patch on ILINE 409 and a shallow approx. NW–SE-oriented channel

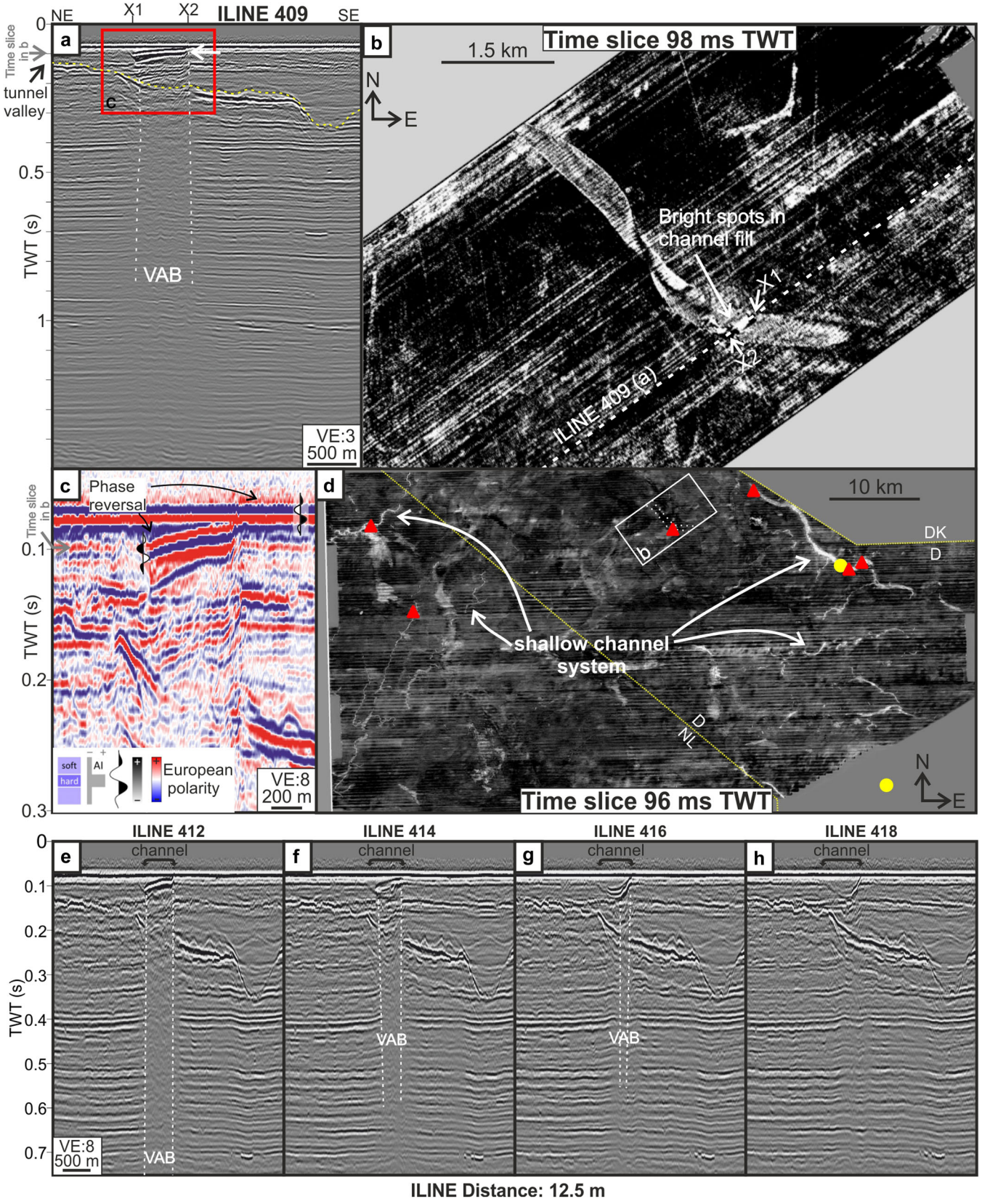

Figure 2. Vertical acoustic blanking (VAB) occurrence in the Ducks Beak imaged by 3D seismic data. (a) VAB correlates with a high-amplitude, dipping reflection. (b) The high-amplitude reflection visible in (a) forms a bright spot within a shallow channel visible in the time slice of the GeoBaSIS-3D data. (c) Enlargement of (a) with different color bar and vertical exaggeration to enhance visibility of the high-amplitude reflection. Note the phase reversal of the high-amplitude reflection within the channel compared to the seafloor reflection. (d) Time slice of the ES2002 survey showing additional meandering channels that are part of a larger tidal or fluvial channel system. White rectangle denotes coverage of GeobaSIS-3D data shown in (b). Dotted line indicates the channel identified in (b). (e–h) Change of the appearance of the VAB feature shown in (a) in ILINE direction of the GeoBaSIS.3D data. Note the changing character of the bright spot within the channel and correlating decrease in VAB. ILINE distance is 12.5 m, and thus 25 m distance between each panel. ILINE numbers increase towards the southeast, so panels (e)–(h) are located closely southeast from ILINE 409 shown in by the dashed line in (b). See Figure 1 for regional location and VAB categories. [Color figure can be viewed at wileyonlinelibrary.com]

(compare locations X1 and X2 in Figure 2a, b). Within this channel, a distinct bright spot is visible (Figure 2b). Note the phase reversal of the high-amplitude, dipping reflection located within the channel compared to the seafloor reflection (Figure 2c). Further VAB occurrences correlate with additional channels at almost identical depth visible in the time slice (96 ms TWT) of the Entenschnabel 2002 3D survey (Figure 2d). The broader spatial coverage provided by this survey unveils the meandering nature of individual channels, indicative of a tidal or fluvial origin. Notably, these individual channels often interconnect, forming a more extensive regional channel system with tributaries or distributary channels (Figure 2d). However, the shallow channel observed in Figure 2b is not discernible, probably due to the superior spatial and vertical resolution of the GeoBaSIS-3D survey. When comparing additional sections from neighboring inlines of the GeoBaSIS-3D data, the strong spatial correlation between the presence and character of the bright spot visible within the surficial channel and the underlying VAB becomes clear as the blanking is always directly below the channel (Figure 2e–h). Over a relatively short distance of 75 m, the spatial extent of the bright spot decreases until it is no longer distinguishable (Figure 2e–h). The area affected by VAB underneath likewise decreases until no blanking is observable (Figure 2e–h). Dipping reflections forming the channel as such are still imaged, but an amplitude anomaly within the channel and below is no longer visible in the last panel (Figure 2h).

In the eastern prolongation of the shallow channel detected by the 3D data (Figure 2), a 2D seismic line also images a VAB feature (Figure 3). The patch of strong amplitude attenuation is about 250 m wide and affects the entire section from just below the seafloor to more than 2 s TWT (Figure 3a). Immediately below the seafloor, the section shows a high-amplitude, dipping reflection, strongly resembling the structure in Figure 2. Likewise, the high-amplitude reflection is phase reversed compared to the seafloor (Figure 3a). Based on the similarity and location of the 2D line, this is most likely the prolongation of the shallow channel identified in the 3D data (see inset map in Figure 3). The panels in Figure 3 display a 2D stacked section with varying maximum offset, thus simulating imaging of the VAB feature with varying active cable lengths during acquisition (Figure 3a–d). Applied processing steps and parameters, such as multiple attenuation, noise reduction, gaining and the used velocity field are identical for all panels. At small maximum offsets, we observe clear VAB from below the high-amplitude reflection across the entire record (Figure 3a). Within the VAB patch, the amplitude of several reflections is strongly attenuated compared to the adjacent area, where the seismic image shows a well-stratified, continuous reflection pattern (see black arrows in Figure 3a). At larger maximum offsets, VAB partially disappears and some reflections in the deeper region (below about 500 ms TWT) are continuous and the amplitudes are barely attenuated (compare black arrows in Figure 3a–d). Note that with a maximum offset of 1000 m, amplitudes in the central part of the former VAB patch no longer appear attenuated (white dotted ellipsis in Figure 3d), while minor residual blanking is observable adjacent to this area. Thus, the extent of VAB in the seismic images shows a clear offset dependency. The reduction of blanking below the channel with increasing offset indicates a shallow origin of the blanking that can be undershot when sufficiently large offsets are available (Figure 3e). Due to the acquisition geometry, raypaths imaging strata directly below the central part of the channel are more prone for undershooting while either upgoing or downgoing rays imaging strata below the flanks of the channel might still cross the shallow channel (Figure 3e). This explains the observation of less amplitude reduction in the central part of the former VAB patch with increasing offset.

Interpretation of the channel infill

The sediment echosounder sections visualize the shallow sedimentary infill of the channels and enable mapping of the channel beyond the coverage of the 3D survey (Figure 4). Based on distinctive reflection patterns, four primary seismic units are identified (U1 to U4 in Figure 4). Figure 4a depicts the channel configuration in proximity to the identified bright spot, representing an almost straight segment of the channel (Figure 4d). The uppermost layer, which is ~1.5 m thick and bounded at the top by the modern seafloor, exhibits a horizontal, high-frequency reflection pattern (U1). The channel in the central part is characterized by a U-shaped syncline with well-stratified sedimentary infill (U2). The southwestern and northwestern portions of the profile reveal two relatively thin underlying layers with more transparent internal reflection patterns and a predominantly horizontal, partly hummocky base (U3).The uppermost channel fill exhibits high-frequency reflections that dip slightly towards the center, displaying a toplap termination towards the overlying units U1 and U3. The deeper channel infill shows lower frequencies but still presents a well-stratified reflection pattern with intermediate transparent layers (Figure 4a). Unit U4 displays less stratification and a disrupted, hummocky reflection pattern. A prominent, nearly horizontal reflection at ~82 ms TWT is disrupted by the channel deposits (Figure 4a). Blanking is noticeable at the channel flanks, represented by strongly attenuated amplitudes that hinder the tracing of reflections (Figure 4a and enlargements a1 and a2). These areas are bound at the top by unit U3 (Figure 4a and enlargements a1 and a2).

The northwestern and southeastern prolongations of the channel are visualized in Figures 4b and 4c respectively. These channel segments are located across a river bend. Units U1, U3 and U4 exhibit similar characteristics. In Figure 4b, unit U3 is only present at the southwestern flank of the channel. In this profile, the channel displays a steep southwestern flank and a northwestern slope that ranges from steep to relatively flat in the shallow portion (U2, Figure 4b). The sedimentary infill exhibits a well-stratified reflection pattern with intermediate, more transparent layers. Reflections are oblique and dip towards the northeast, with toplap terminations towards the overlying base of unit U1. A patch of VAB is situated at the southwestern flank of the channel (Figure 4b and enlargement b1). Here, the VAB is bound at the top by nearly horizontal, slightly hummocky, high-amplitude reflections (dashed yellow line in enlargement b1, Figure 4). In Figure 4c, the internal fill of the channel can be divided into two subunits. The upper subunit, U2a, displays high-amplitude reflections and is well stratified. Reflections are oblique and dip towards the southeast, with a decreasing dip in the shallower section where the reflections become subparallel to the seafloor (Figure 4c). Reflections from subunit U2b exhibit low amplitudes and dip steeply towards the northwest (Figure 4c).

We are aware that amplitude anomalies at the flanks of channels could also originate from the steepness of the reflections. The reason for this is that recording the signal from strongly inclined reflectors is challenging with sediment echosounder data. However, to visualize the channel infill, the images are highly vertically exaggerated, and thus, in reality, the reflectors are still relatively flat. At the northeastern channel flank, blanked reflections dip ~2.7°; notably, just right of the VAB zone, reflections with very similar dip are properly imaged (Fig. 4a1) proving that the blanking is an effect originating from the subsurface characteristics and not from methodological limitations. In the case of Fig. 4b1, the dip of the reflections within the VAB patch is even below that (~1.1°). However, the reflections at

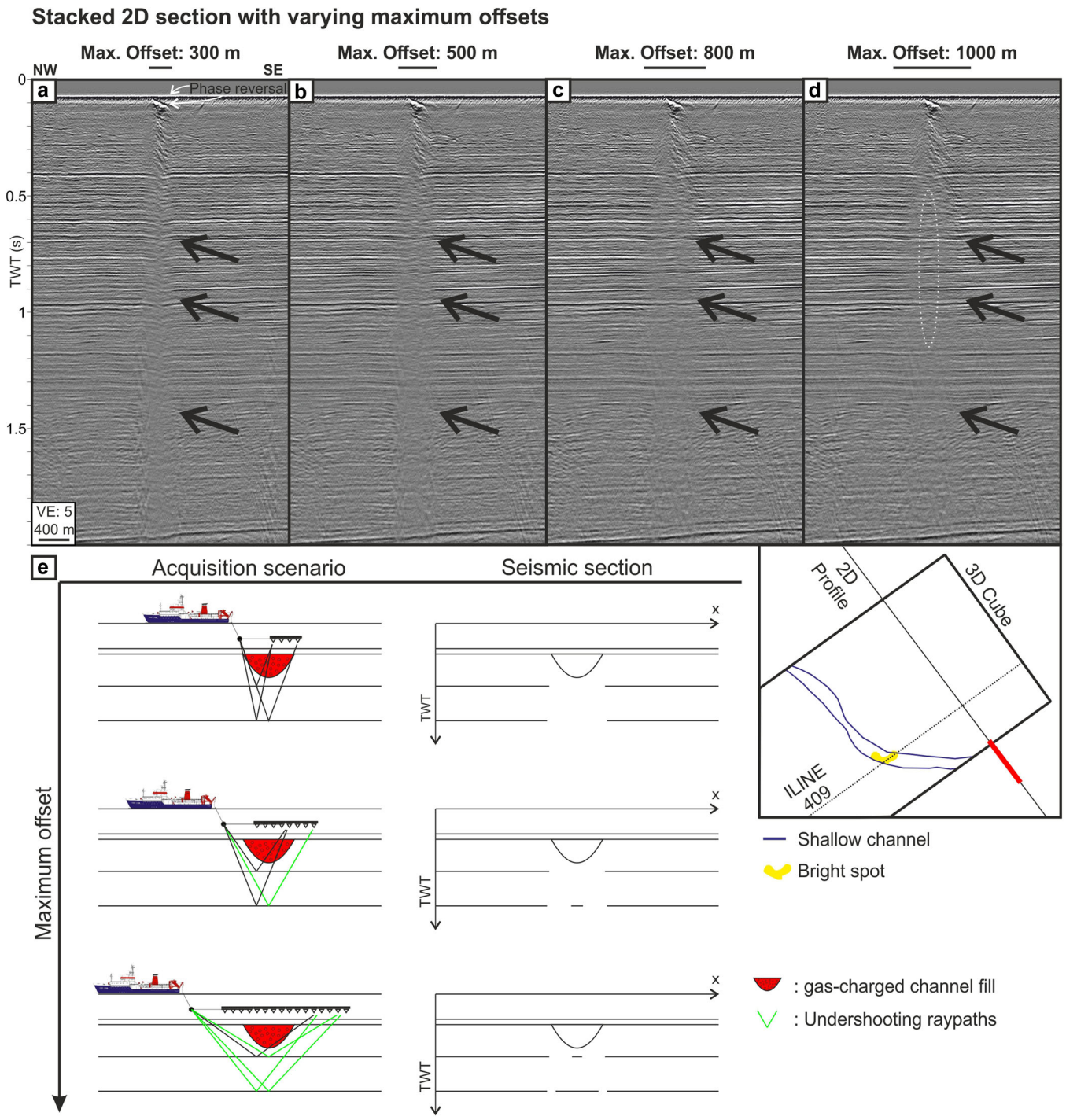

Figure 3. Offset-dependent imaging of VAB feature visible in a 2D seismic section in the eastern prolongation of the shallow channel in Figure 2. Note the similarity of the high-amplitude, phase-reversed reflection directly below the seafloor (a). Panels (a)–(d) show a 2D stacked section with varying maximum offset. Note the decrease of VAB, and thus more continuous imaging of reflections within the VAB patch at greater depths with increasing offset (black arrows). (e) Sketch showing influence of offset in imaging VAB structures. With larger maximum offset, undershooting of the gas-charged channel fill becomes possible (green raypaths) allowing imaging of deeper strata below the channel without influence from the channel infill on the seismic signal. Sketch modified from Frahm et al. (2020). [Color figure can be viewed at wileyonlinelibrary.com]

the southwestern channel flank have dips of around 12.8°, and thus the blanking here might be related to imaging problems by the sediment echosounder (Fig. 4a2).

Discussion

Postglacial evolution of Doggerland channels

Recent studies have already revealed the presence of ancient channel systems, which developed since the last glaciation (Weichselian) and shaped the now drowned lowland landscape between England, Germany and Denmark (commonly known as Doggerland, referring to the Doggerbank now submerged below the North Sea) (Gaffney et al., 2009; van Heteren et al., 2014; Hepp et al., 2017; Coughlan et al., 2018; Prins and Andresen, 2019; Andresen et al., 2022). Within the Ducks Beak, identified channels in this study partly coincide with a channel system published by Hepp et al. (2017), which was detected using single-channel boomer data (Figure 5a). The authors concluded that the channels are of fluvial origin and form a river system connecting Doggerland with the Elbe

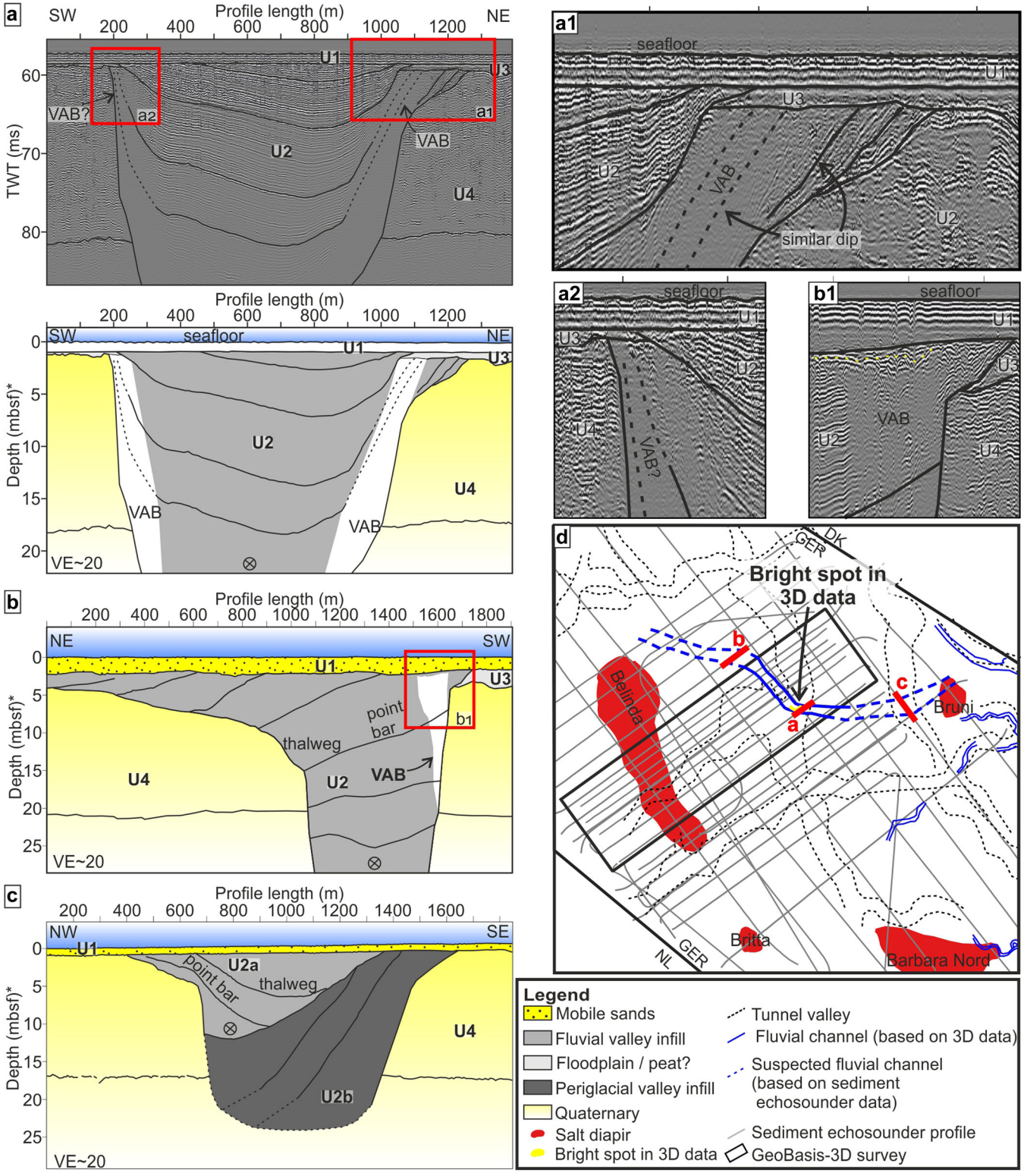

Figure 4. Interpreted sediment echosounder profiles across the investigated incised channel in the Ducks Beak. Interpretation following similar nearby sections published by Hepp et al. (2017). Note the vertical exaggeration of 20 necessary to visualize the incised channels. Depth approximated using a constant sound velocity of 1500 m s^{-1}. Enlarged sections provide insight into the underlying sediment echosounder data quality. For better clarity, only the interpreted sections are shown for sections b and c. An enlarged, high-resolution version of the sections is provided in Supporting Information S3. [Color figure can be viewed at wileyonlinelibrary.com]

Paleovalley. Thus, the rivers were part of the Doggerland drainage system since the last glaciation until the North Sea transgression started to flood the area not later than 9800 years ago (Hepp et al., 2017). The riverine meanders are interpreted to have been subsequently filled with intertidal deposits during transition of the river to an estuary in the course of the marine regression. The additional channels discovered in this work are in agreement with the observations of Hepp et al. (2017), and form part of the westward prolongation of the Doggerland drainage system. In combination with the published incised channels in the Danish, Dutch and British North Sea, the channels detected herein add to a more regional picture of a paleo-riverine landscape (Gaffney et al., 2009; van Heteren et al., 2014; Prins and Andresen, 2019) (Figure 5a).

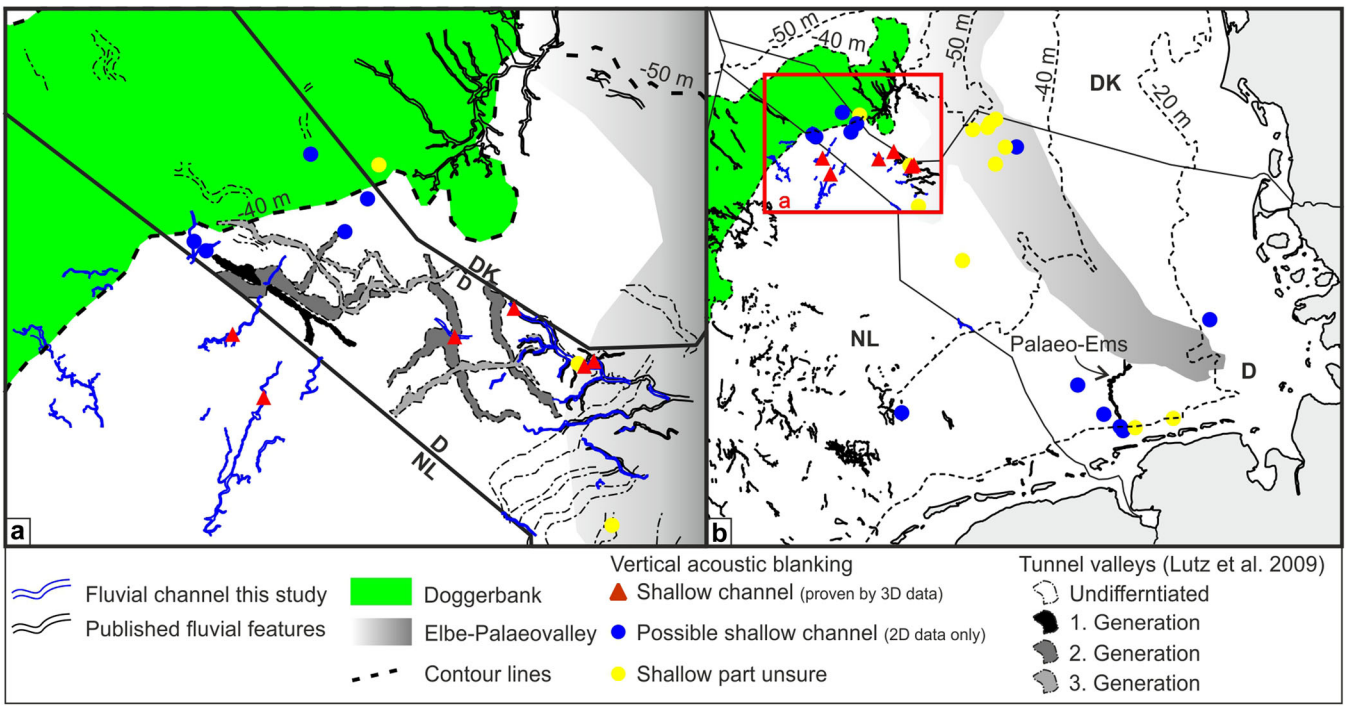

Figure 5. Identified VAB occurrences and shallow incised channels together with published fluvial features including channels, lakes and abandoned river channels within the Ducks Beak (a) and within the overregional setting of the North Sea (Gaffney et al., 2009; van Heteren et al., 2014; Hepp et al., 2017; Prins and Andresen, 2019; EMODnet Geology, 2023). Bathymetric contour lines for −50, −40 and −20 m depth represent hypothetical shorelines at about 10.6, 9.8 and 8.2 ka (Hepp et al., 2017). Outline of Doggerbank and Elbe Paleovalley compiled after Hepp et al. (2017). Note the clustering of VAB occurrences along the channels within the Ducks Beak, within the northeastern Elbe Paleovalley and near the river course of the paleo-Ems. [Color figure can be viewed at wileyonlinelibrary.com]

Stratigraphic interpretation of sediment echosounder profiles is based on characteristic reflection patterns and compared to nearby published sections and sediment cores (Hepp et al., 2017; Coughlan et al., 2018). Overall, the structural style and reflection characteristics are very similar. Accordingly, unit U1 in this work probably represents mobile sands deposited since the last North Sea transgression (Figure 4) (Zeiler et al., 2008; Hepp et al., 2017). Unit U2/U2a marks the channel sedimentary infill, which mostly comprises muddy sands (Figure 3) (Sindowski, 1970; Coughlan et al., 2018), whereas the character of unit U2b is slightly different (Figure 4c). Here, the location of the channel coincides with a known tunnel valley with almost perpendicular strike direction (Figure 4d) (Lutz et al., 2009). Due to their spatial correlation, previous research raised the idea that the Holocene Doggerland drainage partly reused older glacially incised tunnel valleys (Hepp et al., 2017; Prins and Andresen, 2019). The perpendicular strike in this particular case imaged in Figure 3c does not allow this interpretation. However, in cases where the channels closely follow the outline of underlying deeper incising tunnel valleys, these tunnel valleys belong to the third generation based on the age differentiation of Lutz et al. (2009) (Figure 5a). Older tunnel valleys of the first and second generation partly strike perpendicular to the channels identified here (Figures 4c, d and 5a). Possibly, significant topography had already been leveled after the first two generations were formed, so that the formation of the river valleys was influenced only by the tunnel valleys of the third generation. However, this remains rather speculative and needs further investigations and larger scale dating of the tunnel valleys. A relatively prominent more horizontal reflection marks the base of unit U3 located at the flanks of the incised channel. The location and partial overlap of this unit with the channel deposits suggests that this unit represents floodplain or marsh deposits (Figure 4) (Hepp et al., 2017). Unit U4 represents deeper undifferentiated Quaternary deposits. A clear distinction between a fluvial or tidal origin of the channels is not possible due to the lack of sediment cores. We therefore follow the interpretation of previous studies suggesting a fluvial origin of the channels, which were later affected by tidal and marine conditions over the course of the Holocene marine transgression (Hepp et al., 2017; Prins and Andresen, 2019). Overall, the channel configuration with inclined, conformable reflections resembles a thalweg–point bar configuration (Figure 4b, c). Considering the course of the river, the inclined reflections are positioned on the inside of the river bend, consistent with a point bar interpretation (Figure 4). Thereby, the channels are located south of the Dogger Bank, an area with relatively higher topography with regional south to southeast dip (Behre, 2007; EMODnet Bathymetry, 2023). Therefore, the river flow direction was probably from northwest to southeast (Figure 4).

Gas accumulations in postglacial alluvial deposits

This work revealed the correlation of VAB within the German North Sea with shallowly incised channels. Offset-dependent imaging proved that the blanking effect can be reduced or avoided by undershooting if sufficient maximum offset is available (Figure 3). This offset-dependency of the imaged VAB anomalies makes an interpretation of the VAB anomalies as fluid migration pathways implausible and suggests a shallow origin of the VAB related to the incised channels. Similar observations were made in the Dutch North Sea by de Bruin et al. (2022) concerning bright spots at greater depths. de Bruin et al. (2022) analyzed blanking effects below bright spots related to gas accumulations in Cenozoic deltaic deposits. The blanking below the bright spots, referred to as transmission effect, resemble gas chimneys suggesting a fluid migration pathway and corresponding interpretation of a sourcing of the

Cenozoic gas accumulations from deeper strata. However, seismic images of the same location recorded with different acquisition parameters (cable length of 8000 m vs. 2400 m) showed that the transmission effect in the image with 8000-m cable length vanished revealing continuous reflections below the bright spots (de Bruin et al., 2022). The authors concluded that the high maximum offset allowed undershooting of the Cenozoic reservoir and that a fluid migration pathway from the deeper subsurface should be visible on both surveys. Accordingly, the blanking is interpreted as an imaging artifact and the gas was generated *in situ* in the Cenozoic strata (de Bruin et al., 2022).

Locally trapped gas within the channels is a potential explanation of the observed blanking. The presence of gas is in agreement with the observed phase-reversed, high-amplitude reflections within the channel (Figure 2). The gas-charged sediments cause high absorption of acoustic energy strongly reducing signal penetration of the subsurface (Judd and Hovland, 1992). As the blanking below the channels is unmasked as an imaging artifact (see 'VAB distribution and appearance'), no indications for fluids or a migration pathway from the deeper subsurface towards the channel is visible in the seismic data (e.g. bright spots or faults below the channels). Therefore, a thermogenic origin of the gas is unlikely. In contrast, a biogenic gas origin by *in situ* bacterial activity seems more plausible. A high input of organic matter into the Doggerland rivers is likely, as the now submerged lowlands were fertile grasslands, scrup and peatlands (Gaffney et al., 2009; Blumenberg et al., 2022). Biomarker and gas geochemical analyses of peat cores near the channels identified here within the Ducks Beak proved methane enrichments of 'Doggerland' peat layers with a probable biogenic methane origin (Blumenberg et al., 2022).

However, the blanking is only detected at specific sites along the channels (Figure 2). Possibly, biogenic gas generated within the fluvial or tidal deposits simply escaped in most cases while only at selected locations, some form of barrier trapped gas within the sediments leading to sufficient accumulation to produce the blanking effect on seismic data. Fine-grained muds from meadow or floodplain deposits at the river flanks could form this barrier if the porosity contrast between them and underlying gas-bearing sediments is sufficiently high (Garcia-Gil et al., 2002). In Figure 4a, the horizontal subunit U3 at the flanks of the channel, which we interpreted as floodplain deposits, could form such a barrier. Although Figure 4b shows similar floodplain deposits, these do not directly overlie the VAB patch. However, such deposits do not exist everywhere in the study area. We surmise that the occurrence of gas depends on both the amount of gas that is being produced, the permeability of the sediments that control the gas to migrate to the seafloor and local barriers. Studies of gas accumulations in the Baltic Sea have shown that the balance of gas production and gas migration controls whether significant gas accumulations can build up (Lohrberg et al., 2020).

Shallow gas accumulation was not necessarily solely within the channels, but might also simply be trapped within the uppermost sedimentary layers without a connection to the channels, for example as investigated by Tóth et al. (2014) in the Baltic Sea. Below the gas-charged sediments, VAB might also occur with a high-amplitude reflection above originating from the gas front interface. However, this prominent reflection usually has a more horizontal character. Thus, in cases where the VAB is only imaged by 2D seismic data, a correlation to fluvial or tidal channels is uncertain, especially if the shallow subsurface is not well resolved. In this work, VAB occurrences imaged in 2D data, which showed a high-amplitude reflection with visible dip potentially forming a valley-like structure, have been interpreted to indicate an incised channel rather than shallow free gas. However, this needs confirmation by 3D data or closely spaced 2D seismic and hydroacoustic profiles.

In conclusion, the occurrences of VAB anomalies detected in this study are probably caused by a biogenic gas-charged sedimentary infill of shallow fluvial or tidal channels located directly below the seafloor. The gas-charged sediments attenuate acoustic energy and hamper signal penetration. Thus, the resulting discontinuous seismic image below the shallow channel represents an imaging artifact.

In principle, the occurrences of VAB identified in this work cluster in two principal regions (Figure 1). Most VAB anomalies are located within the Ducks Beak and correlate with the ancient Doggerland fluvial system as discussed above (Figure 5a). Additionally, many of the occurrences in the northern North Sea lie within the northwestern part of the Elbe- Paleovalley, close to the German–Danish maritime border (Figure 5b). The other cluster is located in the northern extension of the present Ems Estuary, in direct proximity to the published course of the paleo-Ems (Figure 5b) (Hepp et al., 2017). This demonstrates the possibility of using the detection of VAB anomalies in large-scale datasets with other original targets (e.g. from the hydrocarbon industry) to identify former river channels or other features of paleo-landscapes such as lakes or deltas. Thereby, the results of this study extend the understanding of the complex drowned landscapes of the present North Sea and generally agree well with the understanding of Doggerland as a coastal lowland with abundant hunting game and fishing opportunities in rivers and shallow marine waters (Gaffney et al., 2009). In this sense, the VAB anomalies could serve as a spotlight to identify such paleo-landscape structures and thus point to areas for smaller scale analysis and further investigation. This may be an interesting approach for geoarcheology and future research on prehistoric hunter-gatherer societies living in the area of the present-day North Sea and worldwide. Additionally, shallow gas marks a hazard for drilling or construction, such as for offshore wind farms. Accordingly, the identification of VAB anomalies can provide input for hazard assessments in planning of such projects.

Conclusions

This study analyzes and maps VAB anomalies in seismic data from the German North Sea sector to identify if observed patches of VAB represent genuine geological structures or if they are merely seismic artifacts masking underlying signals. Analysis of a comprehensive database consisting of 2D and 3D seismic data in combination with sediment echosounder data sheds light on the origin and nature of these VAB anomalies. The results of the study revealed multiple occurrences of VAB distributed across the North Sea in patches of varying widths mostly affecting the seismic record from directly below the seafloor to 1–2 s TWT (Figure 1). These VAB patches often correlate with valley-like structures characterized by slightly dipping, phase-reversed, high-amplitude reflections. The analysis of the 3D seismic data from the Ducks Beak area ('Entenschnabel') reveals a clear correlation between VAB anomalies and bright spots within shallow incised channels (Figure 2). Offset-dependent imaging shows that the channels can be undershot and showed continuous reflections below the channel unaffected by blanking (Figure 3). Sediment echosounder data visualize the sedimentary infill of these channels including thalweg and point bar geometries (Figure 4). The findings of the study suggest that the VAB anomalies are associated with fluvial or tidal channel systems that developed since the last glaciation in the now-drowned

lowland landscape between England, Germany and Denmark known as Doggerland (Figure 5). The observed blanking is probably caused by high absorption of acoustic energy due to shallow biogenic gas trapped within the channels, potentially due to accumulation below more fine-grained floodplain deposits. Accordingly, the vertical blanking and discontinuous seismic image below the shallow channel represents an imaging artifact.

VAB occurrences cluster in two principal areas in the North Sea (Figure 5): the first group is located within the Ducks Beak and northern German North Sea and can be associated with the ancient drainage system of Doggerland and the Elbe Paleovalley, while in the second area, VAB occurrences group along the course of the paleo-Ems (Figure 5). Therefore, the identification of VAB anomalies in large-scale datasets (e.g. from the oil and gas industry) can serve as a spotlight to identify unknown paleo-river channels and new research opportunities, such as for paleo-landscape reconstruction and geoarcheology. Additionally, the improved understanding of acoustic blanking in seismic data provided by this study helps to avoid misinterpretation of such features as gas chimneys or other fluid migration pathways.

Acknowledgements. The authors would like to thank the editor Achim Brauer and the reviewers Peter Feldens and Mads Huuse for their constructive comments and remarks. Further, the authors acknowledge the financial support from the Federal Ministry of Education and Research of Germany (BMBF) in the framework of GEOSTOR: Kohlendioxidspeicherung in geologischen Formationen der deutschen Nordsee (project number 03F0893B), one of the six research consortia of the German Marine Research Alliance (DAM) research mission 'Marine carbon sinks in decarbonization pathways'. We thank AspenTech for providing Paradigm/EPOS Software Package licenses via the Academic Software Program (https://www.aspentech.com/en/academic-program) to support BGR as a national geological service in non-profit work for the public and education. This will enable BGR to develop a variety of digital products on the subsurface and make them available. The authors declare that they have no known competing financial interests or personal relationships that could have appeared to influence the work reported in this paper. Open Access funding enabled and organized by Projekt DEAL.

Data availability statement

Used data from the German North Sea are available under the framework of the GeoIDG and can be requested via https://geoportal.bgr.de/. Seismic data from the Dutch North Sea are accessible via www.nlog.nl.

Supporting information

Additional supporting information can be found in the online version of this article.

Abbreviations. BGR, Bundesanstalt für Geowissenschaften und Rohstoffe/Federal Institute for Geoscience and Natural Resources; CCS, carbon capture and storage; SRME, surface related multiple attenuation; TWT, two-way travel time; VAB, vertical acoustic blanking; VE, vertical exaggeration.

References

Ahlrichs, N., Noack, V., Hübscher, C., Seidel, E., Warwel, A. & Kley, J. (2021) Impact of Late Cretaceous inversion and Cenozoic extension on salt structure growth in the Baltic sector of the North German Basin. *Basin Research*, 34, 220–250.

Andresen, K.J., Hepp, D.A., Keil, H. & Spiess, V. (2022) *Seismic morphologies of submerged late glacial to Early Holocene landscapes at the eastern Dogger Bank, central North Sea Basin – implications for geo-archaeological potential*. London: Geological Society Special Publications 525.

Armstrong, T., McAteer, J. & Connolly, P. (2001) Removal of overburden velocity anomaly effects for depth conversion. *Geophysical Prospecting*, 49, 79–99.

Bachmann, G.H., Geluk, M., Warrington, G., Becker-Roman, A., Beutler, G., Hagdorn, H. et al. (2010) Triassic. In: Doornenbal, H., & Stevenson, A.G. (Eds.) *Petroleum Geological Atlas of the Southern Permian Basin Area*. Houten: EAGE Publications. pp. 149–173.

Behre, K.-E. (2007) A new Holocene sea-level curve for the southern North Sea. *Boreas*, 36, 82–102.

Blumenberg, M., Schlömer, S., Reinhardt, L., Scheeder, G., Pape, T. & Römer, M. (2022) Biomarker insights into a methane-enriched Holocene peat-setting from "Doggerland" (central North Sea). *The Holocene*, 32, 1015–1025.

Böttner, C., Berndt, C., Reinardy, B.T.I., Geersen, J., Karstens, J., Bull, J.M. et al. (2019) Pockmarks in the Witch Ground Basin, Central North Sea. *Geochemistry, Geophysics, Geosystems*, 20, 1698–1719.

Breuer, S., Bebiolka, A., Noack, V. & Lang, J. (2023) The past is the key to the future—considering Pleistocene subglacial erosion for the minimum depth of a radioactive waste repository. *E&G Quaternary Sci. J*, 72, 113–125.

Callow, B., Bull, J.M., Provenzano, G., Böttner, C., Birinci, H., Robinson, A.H. et al. (2021) Seismic chimney characterisation in the North Sea—Implications for pockmark formation and shallow gas migration. *Marine and Petroleum Geology*, 133, 105301.

Cameron, T.D.J., Bulat, J. & Mesdag, C.S. (1993) High resolution seismic profile through a Late Cenozoic delta complex in the southern North Sea. *Marine and Petroleum Geology*, 10, 591–599.

Coughlan, M., Fleischer, M., Wheeler, A.J., Hepp, D.A., Hebbeln, D. & Mörz, T. (2018) A revised stratigraphical framework for the Quaternary deposits of the German North Sea sector: a geological-geotechnical approach. *Boreas*, 47, 80–105.

de Bruin, G., Ten Veen, J., Wilpshaar, M., Versteijlen, N., Geel, K., Verweij, H. et al. (2022) Origin of shallow gas in the Dutch North Sea—Seismic versus geochemical evidence. *Interpretation*, 10, SB63–SB76.

de Jager, J. (2003) Inverted basins in the Netherlands, similarities and differences. *Netherlands Journal of Geosciences - Geologie en Mijnbouw*, 82, 339–349.

Ehlers, J. (1990) Reconstructing the dynamics of the North-west European Pleistocene ice sheets. *Quaternary Science Reviews*, 9, 71–83.

Ehrhardt, A., Albers, A., Behrens, T., Demir, Ü., Ebert, T., Engels, M. et al. 2021. GeoBaSIS-3D: Geophysical Investigations for Barrier Structures and their Integrity in the subsurface of the German Nort Sea by means of 3D-Seismic data, Cruise NO. MSM100, Maria S. Merian - Berichte. Begutachtungspanel Forschungsschiffe, p. 55.

EMODnet Bathymetry. 2023. EMODnet Bathymetry—Depth, EMODnet Map Viewer.

EMODnet Geology. 2023. EMODnet Geology—Submerged landscapes, EMODnet Map Viewer.

Frahm, L., Hübscher, C., Warwel, A., Preine, J. & Huster, H. (2020) Misinterpretation of velocity pull-ups caused by high-velocity infill of tunnel valleys in the southern Baltic Sea. *Near Surface Geophysics*, 18, 643–657.

Gaffney, V., Fitch, S. & Smith, D. 2009. Europe's Lost World: The Rediscovery of Doggerland, Reseach Report, York.

Garcia-Gil, S., Vilas, F. & Garcia-Garcia, A. (2002) Shallow gas features in incised-valley fills (Ría de Vigo, NW Spain): a case study. *Continental Shelf Research*, 22, 2303–2315.

Hepp, D.A., Warnke, U., Hebbeln, D. & Mörz, T. (2017) Tributaries of the Elbe Palaeovalley: Features of a Hidden Palaeolandscape in the German Bight, North Sea. In: Bailey, G.N., Harff, J. & Sakellariou, D. (Eds.) *Under the Sea: Archaeology and Palaeolandscapes of the Continental Shelf*. Cham: Springer International Publishing. pp. 211–222.

Hughes, A.L.C., Gyllencreutz, R., Lohne, Ø.S., Mangerud, J. & Svendsen, J.I. (2016) The last Eurasian ice sheets – a chronological database and time-slice reconstruction, DATED-1. *Boreas*, 45, 1–45.

Huuse, M. (2000) Overdeepened Quaternary valleys in the eastern Danish North Sea: morphology and origin. *Quaternary Science Reviews*, 19, 1233–1253.

Judd, A.G. & Hovland, M. (1992) The evidence of shallow gas in marine sediments. *Continental Shelf Research*, 12, 1081–1095.

Karstens, J. & Berndt, C. (2015) Seismic chimneys in the Southern Viking Graben—Implications for palaeo fluid migration and overpressure evolution. *Earth and Planetary Science Letters*, 412, 88–100.

Kley, J. & Voigt, T. 2008. Late Cretaceous intraplate thrusting in central Europe: Effect of Africa-Iberia-Europe convergence, not Alpine collision. Geology 36.

Kristensen, T.B., Huuse, M., Huuse, M., Redfern, J., Heron, D.P.L., Dixon, R.J. et al. (2012) Multistage erosion and infill of buried Pleistocene tunnel valleys and associated seismic velocity effects, Glaciogenic Reservoirs and Hydrocarbon Systems. Geological Society of London, p. 0.

Laier, T. & Jensen, J.B. (2007) Shallow gas depth-contour map of the Skagerrak-western Baltic Sea region. *Geo-Marine Letters*, 27, 127–141.

Lohrberg, A., Schmale, O., Ostrovsky, I., Niemann, H., Held, P. & Schneider von Deimling, J. (2020) Discovery and quantification of a widespread methane ebullition event in a coastal inlet (Baltic Sea) using a novel sonar strategy. *Scientific Reports*, 10, 4393.

Lutz, R., Gaedicke, C., Lutz, R. & Winsemann, J. (2009) Pleistocene tunnel valleys in the German North Sea: spatial distribution and morphology. *Zeitschrift der Deutschen Geologischen Gesellschaft*, 160, 225–235.

Mathys, M., Thießen, O., Theilen, F. & Schmidt, M. (2005) Seismic Characterisation of Gas-rich Near Surface Sediments in the Arkona Basin, Baltic Sea. *Marine Geophysical Researches*, 26, 207–224.

Müller, S., Reinhardt, L., Franke, D., Gaedicke, C. & Winsemann, J. (2018) Shallow gas accumulations in the German North Sea. *Marine and Petroleum Geology*, 91, 139–151.

Okyar, M. & Ediger, V. (1999) Seismic evidence of shallow gas in the sediment on the shelf off Trabzon, southeastern Black Sea. *Continental Shelf Research*, 19, 575–587.

Overeem, I., Weltje, G.J., Bishop-Kay, C. & Kroonenberg, S.B. (2001) The Late Cenozoic Eridanos delta system in the Southern North Sea Basin: a climate signal in sediment supply? *Basin Research*, 13, 293–312.

Peryt, T.M., Geluk, M., Mathiesen, A., Paul, J. & Smith, K. (2010) Zechstein. In: Doornenbal, J.C. & Stevenson, A.G. (Eds.) *Petroleum Geological Atlas of the Southern Permian Basin Area*. Houten: EAGE Publications. pp. 123–147.

Pharaoh, T., Dusar, M., Geluk, M., Kockel, F., Krawczyk, C., Krzywiec, P. et al. (2010) Tectonic evolution. In: Doornenbal, H. & Stevenson, A.G. (Eds.) *Petroleum Geological Atlas of the Southern Permian Basin Area*. Houten: EAGE Publications. pp. 25–57.

Piotrowski, J.A. (1994) Tunnel-valley formation in northwest Germany—geology, mechanisms of formation and subglacial bed conditions for the Bornhöved tunnel valley. *Sedimentary Geology*, 89, 107–141.

Prins, L.T. & Andresen, K.J. (2019) Buried late Quaternary channel systems in the Danish North Sea—Genesis and geological evolution. *Quaternary Science Reviews*, 223, 105943.

Schroot, B.M. & Schüttenhelm, R.T.E. (2003) Expressions of shallow gas in the Netherlands North Sea. *Netherlands Journal of Geosciences—Geologie en Mijnbouw*, 82, 91–105.

Sindowski, K.-H. (1970) Das Quartär im Untergrund der Deutschen Bucht (Nordsee). *E&G—Quaternary Science Journal*, 21, 33–46.

Thöle, H., Gaedicke, C., Kuhlmann, G. & Reinhardt, L. (2014) Late Cenozoic sedimentary evolution of the German North Sea—A seismic stratigraphic approach. *Newsletters on Stratigraphy*, 47, 299–329.

Tóth, Z., Spieß, V. & Jensen, J. (2014) Seismo-acoustic signatures of shallow free gas in the Bornholm Basin, Baltic Sea. *Continental Shelf Research*, 88, 228–239.

Trampe, A.F., Lutz, R., Franke, D. & Bücker, C. (2014) Aktuelle Untersuchungen anhand seismischer Daten [Shallow Natural Gas in the German North Sea]. *Erdöl, Erdgas, Kohle*, 130, 1–3.

Tucker, M.E. (1991) Sequence stratigraphy of carbonate-evaporite basins: models and application to the Upper Permian (Zechstein) of northeast England and adjoining North Sea. *Journal of the Geological Society*, 148, 1019–1036.

Underhill, J.R. & Partington, M.A. (1993) Jurassic thermal doming and deflation in the North Sea: implications of the sequence stratigraphic evidence. Geological Society, London, Petroleum Geology Conference series 4, 337-345.

van Heteren, S., Meekes, J.A.C., Bakker, M.A.J., Gaffney, V., Fitch, S., Gearey, B.R. et al. (2014) Reconstructing North Sea palaeolandscapes from 3D and high-density 2D seismic data: An overview. *Netherlands Journal of Geosciences - Geologie en Mijnbouw*, 93, 31–42.

Vejbæk, O.V. (2002) Post mid-Cretaceous inversion tectonics in the Danish Central Graben - regionally synchronous tectonic events? *Bulletin of the Geological Society of Denmark*, 49, 129–144.

Warsitzka, M., Jähne-Klingberg, F., Kley, J. & Kukowski, N. (2019) The timing of salt structure growth in the Southern Permian Basin (Central Europe) and implications for basin dynamics. *Basin Research*, 31, 337–360.

Zeiler, M., Schwarzer, K. & Ricklefs, K. (2008) Seabed Morphology and Sediment Dynamics. *Die Küste*, 74, 31–44.

Ziegler, P.A. (1990) Tectonic and paleogeographic development of the North Sea Rift System. In: Blundell, D. & Gibbs, A.D. (Eds.) *Tectonic Evolution of North Sea Rifts*. New York: Oxford University Press. pp. 1–36.